THE INFLUENCE OF ADVECTION ON THE SHORT TERM CO_2-BUDGET IN AND ABOVE A FOREST CANOPY

C. FEIGENWINTER[1,★], C. BERNHOFER[2] and R. VOGT[1]
[1]*Institute of Meteorology, Climatology and Remote Sensing, University of Basel, Klingelberstrasse 27, CH-4056 Basel, Switzerland;* [2]*Institute of Hydrology and Meteorology, Dresden University of Technology, Germany*

(Received in final form 12 January 2004)

Abstract. An experimental micrometeorological set-up was established at the CARBOEUROFLUX site in Tharandt, Germany, to measure all relevant variables for the calculation of the vertical and horizontal advective fluxes of carbon dioxide. The set-up includes two auxiliary towers to measure horizontal and vertical CO_2 and H_2O gradients through the canopy, and to make ultrasonic wind measurements in the trunk space. In combination with the long-term flux tower an approximately even-sided prism with a typical side-length of 50 m was established. It is shown that under stable (nighttime) conditions the mean advective fluxes have magnitudes on the same order as the daily eddy covariance (EC) flux, which implies that they play a significant, but not yet fully understood, role in the carbon budget equation. The two advective fluxes are opposite and seem to cancel each other at night (at least for these measurements). During the day, vertical advection tends to zero, while horizontal advection is still present implying a flow of CO_2 out of the control volume. From our measurements, a mean daily gain of 2.2 gC m^{-2} d^{-1} for the horizontal advection and a mean daily loss of 2.5 gC $m^{-2}d^{-1}$ for the vertical advection is calculated for a period of 20 days. However the large scatter of the advective fluxes has to be further investigated. It is not clear yet whether the large variability is natural or due to measurement errors and conceptual deficiencies of the experiment. Similar results are found in the few comparable studies.

Keywords: Advection, Carbon sequestration, CO_2, Forest ecosystems.

1. Introduction

In the recent past, long-term carbon flux networks have been established in Europe (EUROFLUX, CARBOEUROFLUX, i.e., Valentini et al., 1996, 2000; see also http://www.bgc-jena.mpg.de/public/carboeur/) and in the Americas (AMERIFLUX, see also http://public.ornl.gov/ameriflux/) to enhance our knowledge of terrestrial carbon exchanges. In the late 1990s these efforts were embedded in the worldwide FLUXNET (Baldocchi et al., 2000; special issue FLUXNET 2000 synthesis, *Agric. For. Meteorol.*, **113**, 2002; see also http://www.eosdis.ornl.gov/FLUXNET/). The flux networks mentioned above usually ignore the advective terms of the

★ E-mail: feigenwinter@metinform.ch

Boundary-Layer Meteorology **113:** 201–224, 2004.

conservation equation and determine net ecosystem exchange (NEE), by using the eddy covariance (EC) method (Moncrieff et al., 1997; Aubinet et al., 2000), which relies on the measurement of the turbulent vertical flux of CO_2 above the canopy, and the carbon storage change in the layer below the eddy flux sensors. (NEE also can be evaluated using biometric methods.) Missing data due to instrument errors or conditions in which the EC method is questionable (i.e., under stable nighttime conditions and weak turbulence or heavy precipitation) are usually corrected by models based on soil temperature, photosynthetically active radiation (PAR) and the so called u_* correction (Goulden et al., 1996; Grünwald and Bernhofer, 2000; Falge et al., 2001a, b). However, the presence of tall vegetation, variable topography, mesoscale heterogeneity and ensuing mean vertical flow creates complications that were recently addressed by Lee (1998), Bernhofer and Vogt (1999), Finnigan (1999), Paw U et al. (2000), Finnigan et al. (2003) and Aubinet et al. (2003). All of these studies consider the NEE advection terms at forested sites in complex terrain (i.e., tall vegetation, non-flat terrain, heterogeneous canopy, etc.). Especially during stable nighttime conditions, the CO_2 fluxes measured by the EC method are typically underestimated, which can result in an erroneous evaluation of the annual carbon sequestration (Baldocchi et al., 1997; Aubinet et al., 2000; Eugster and Siegrist, 2000; Lee and Hu, 2002). Beside the well-known and largely discussed measurement errors, such as high frequency flux loss caused by EC instrumentation and closed path sensors (Leuning and Moncrieff, 1990; Bernhofer et al., 2003 a, b), low frequency flux loss due to too short an averaging interval (i.e., Massmann and Lee, 2002) and errors in storage measurements, there is evidence that the neglected advective processes are responsible for the underestimation of nighttime fluxes rather than measurement errors (Lee and Hu, 2002; Aubinet et al., 2003).

As a consequence, the experimental set-up of future micrometeorological sites should be designed to account for the entire mass balance in a soil–vegetation–atmosphere volume. This holds especially for typical forest sites with complex topography and limited fetch. It is also a very ambitious challenge, since it requires more than one tower for measurements, which consequently multiplies the costs of infrastructure and instrumentation. Therefore, the optimum design has to be evaluated through short term measurement campaigns.

The central object of our study, in the framework of the AFO 2000 project VERTIKO, is to experimentally evaluate the advective fluxes as a part of the soil–vegetation–atmosphere exchange of trace gases (e.g., carbon dioxide). In this paper the first results of a 3-year project dealing with the influence of surface heterogeneity on advective effects are presented. We restrict ourselves to CO_2 NEE.

2. Theoretical Considerations

For simplicity, the usual symbol convention is adopted here by which t is time, prime denotes the departure from the mean, overbar is the Reynolds averaging operator, brackets $\langle\ \rangle$ stand for an ensemble mean value, which is supposed to be valid for the whole control volume, S_B is the biological source/sink strength term and u, v and w are the wind velocity components in the x (east), y (north) and z (normal to surface) directions, respectively. For carbon dioxide, the mass conservation states that the CO_2 mixing ratio c, defined as the ratio of mole density of CO_2 to the mole density of dry air ρ_c/ρ_a (usually measured in ppm), is balanced by the flux divergence of CO_2 in the x, y and z directions:

$$S_B(t,x,y,z) = \frac{\partial c}{\partial t} + \frac{\partial uc}{\partial x} + \frac{\partial vc}{\partial y} + \frac{\partial wc}{\partial z}. \tag{1}$$

Integration over a control volume of height z_r and a longitudinal and lateral extent of $2L$, after Reynolds averaging, results in (Finnigan, 1999):

$$\frac{1}{4L^2}\int_L\int dx\ dy \int_0^{z_r} dz\ S_B(t,x,y,z) = \frac{1}{4L^2}\int_L\int dx\ dy \times \int_0^{z_r} dz\left(\frac{\partial \bar{c}}{\partial t} + \frac{\partial(\bar{u}_j\bar{c})}{\partial x_j} + \frac{\partial(\overline{u_j'c'})}{\partial x_j}\right), \tag{2}$$

where $x_j \equiv x, y, z$ is the coordinate system, and $u_j \equiv u$, v, w are the associated wind components. Some simplifications to Equation (2) can be made, though they have to be examined critically (Finnigan, 1999; Finnigan et al., 2003). Neglecting the horizontal turbulent flux divergence terms and the horizontal variation of the vertical flux ($\partial\overline{u'c'}/\partial x = \partial\overline{v'c'}/\partial y = \partial\overline{w'c'}/\partial x = \partial\overline{w'c'}/\partial y = 0$), applying continuity ($\partial\bar{u}/\partial x + \partial\bar{v}/\partial y + \partial\bar{w}/\partial z = 0$) and assuming a horizontally homogeneous concentration gradient ($\partial^2\bar{c}/\partial x^2 = \partial^2\bar{c}/\partial y^2 = 0$), Equation (2) reduces to

$$\int_0^{z_r} S_B(t,z)\,dz = \underbrace{\int_0^{z_f} \frac{\partial \bar{c}(z)}{\partial t}\,dz}_{\text{I}} + \underbrace{\int_0^{z_r} \frac{\partial \overline{w'c'}(z)}{\partial z}\,dz}_{\text{II}} + \underbrace{\int_0^{z_r} \bar{w}(z)\frac{\partial \bar{c}(z)}{\partial z}\,dz}_{\text{III}} + \underbrace{\int_0^{z_r}\left(\bar{u}(z)\frac{\partial \bar{c}(z)}{\partial x} + \bar{v}(z)\frac{\partial \bar{c}(z)}{\partial y}\right)dz}_{\text{IV}}. \tag{3}$$

Here, term I is the storage change term and will be calculated from a mean vertical concentration profile. The eddy flux term II on the right-handside (RHS) of Equation (3) can be written as

$$\int_0^{z_r} \frac{\partial \overline{w'c'}(z)}{\partial z}\, dz = \overline{w'c'}(z_r) - \overline{w'c'}(0). \tag{4}$$

Using Lee's (1998) notation for the vertical advection, term III on the RHS of (3), results in

$$\int_0^{z_r} \bar{w}(z) \frac{\partial \bar{c}(z)}{\partial z}\, dz = \bar{w}(z_r)(\bar{c}(z_r) - \langle c \rangle), \tag{5}$$

where

$$\langle c \rangle = \frac{1}{z_r} \int_0^{z_r} \bar{c}(z)\, dz \tag{6}$$

stands for the mean CO_2 concentration in the control volume and Lee's hypothesis of

$$\frac{\partial \bar{w}(z)}{\partial z} = \frac{\bar{w}(z_r)}{z_r} \tag{7}$$

is applied. The problem of finding the appropriate value for the mean vertical velocity is addressed in as Section 4.3.

Term IV on the RHS of Equation (3), the horizontal advection, requires at least two concentration profiles for the analysis, which may be appropriate in terrain where the flow field is mainly two-dimensional (i.e. upslope/downslope flow regime (Aubinet et al., 2003)). However, for a complete three-dimensional analysis, three or more towers are necessary. The procedure of deriving vertical profiles of wind velocity, and especially of the concentration gradient, is a crucial task and has significant impact on the size of this term. Note that a wind perpendicular to the direction of the horizontal gradient will result in a zero advection term.

The source/sink strength S_B of CO_2 including soil respiration is the NEE with flux units of μmol m^{-2} s^{-1}. Mixing ratio therefore has to be multiplied, according to gas laws, by a factor, which is dependent on ambient temperature, pressure and the molar mass of CO_2, to receive a concentration in units of μmol m^{-3}. A first estimate of NEE after all these modifications to Equation (3) results finally in

$$\begin{aligned} \mathrm{NEE} = \int_0^{z_r} S_B(t,z)\, dz + \overline{w'c'}(0) = \frac{\partial \langle c \rangle}{\partial t} + \overline{w'c'}(z_r) + \bar{w}(z_r)(\bar{c}(z_r) - \langle c \rangle) \\ + \int_0^{z_r} \left(\bar{u}(z) \frac{\partial \bar{c}(z)}{\partial x} + \bar{v}(z) \frac{\partial \bar{c}(z)}{\partial y} \right) dz. \end{aligned} \tag{8}$$

The sign convention for all (horizontal and vertical) fluxes is that positive fluxes refer to a transport of CO_2 out of the control volume including fluxes due to storage changes. Positive storage flux represents an additional source of carbon, negative refers to a carbon sink in the control volume. This is in agreement with the definition of NEE as used in the FLUXNET community (Baldocchi et al., 2000; Paw U et al., 2000; Aubinet et al., 2001; Dolman et al., 2002; Saguisa et al., 2002). Since our study concentrates on the advection terms only, data for storage change and especially the EC flux were taken from the work of Grünwald (2002) and the EUROFLUX database.

3. Site and Instrumentation

The measurements described in this study were made at the tower site at Tharandt, Germany, which has been operated by the Institute of Hydrology and Meteorology of the Dresden University of Technology since the late 1950s, the site became part of the EUROFLUX network in 1996. The tower (50°58′ N, 13°34′ E), 375 m a.s.l. is situated in the eastern part of the Tharandt forest (ca. 600 ha) near Dresden at the northern base of the Ore mountains and serves as an anchor station for ecological, hydrological and remote sensing applications. It is also a Global Terrestrial Observing System reference site. The climate is at the transition from maritime to continental temperate conditions (mean annual temperature 7.7 °C, mean annual maximum temperature 28 °C, mean annual minimum temperature −20.6 °C, mean annual precipitation 819 mm). The area around the tower is primarily covered by Norway spruce (*Picea abies*) with a mean canopy height of about 29 m. Figure 1 gives an overview of the land use in the vicinity of the site in 1993. For more detailed information about the site refer to Grünwald (2002).

Leaf area index (LAI) was found to be approximatively 8 in 1999 (Bernhofer et al., 2003a, b), however the site was thinned in spring 2002. The undercover is very sparse, and trunk space reaches up to 12 m where the crown space begins. The principal flux network measurements are from a 42 m tower (denoted as P1). In addition to these measurements, wind vector and CO_2 concentration profiles were measured during the campaign in September/October 2001 at two points (P2 and P3) about 50 m from the main tower in order to probe a triangular prism. Figure 2 gives an overview of the experimental set-up, and the instrumentation is listed in Table I.

4. Methods

In our campaign, we tried a relatively inexpensive set-up using small towers (up to 3 m a.g.l.) and trees (for the 8 and 26 m levels) instead of tall towers to

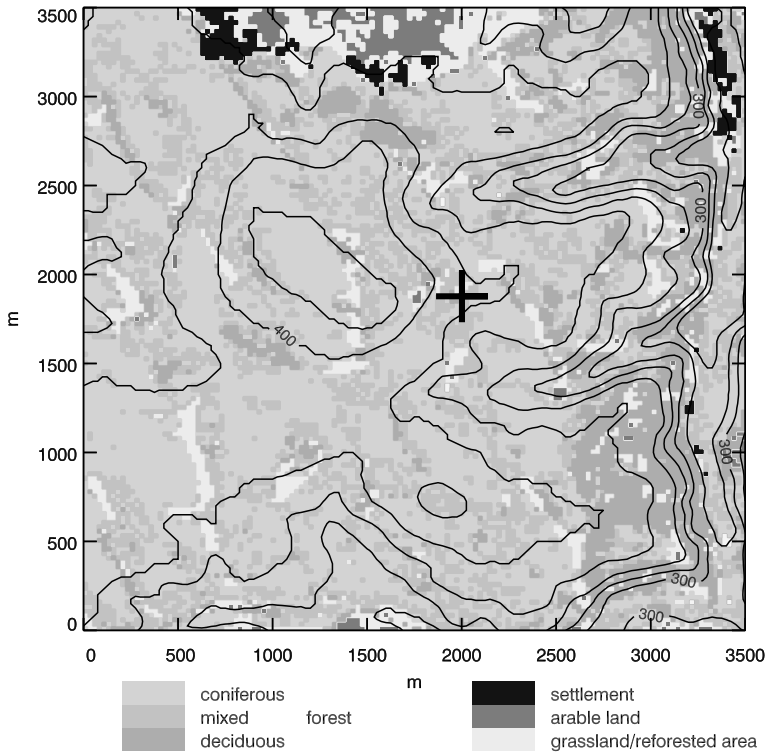

Figure 1. Land use surrounding the Tharandt site (+, 50°58′ N, 13°34′ E). The contour interval is 20 m.

measure all relevant variables for the calculation of the additional advection terms for the evaluation of NEE.

4.1. CO_2 DATA ACQUISITION AND VERTICAL CONCENTRATION PROFILES

Profiles of CO_2 concentrations at every edge of the prism were measured by closed path infrared gas analysers (IRGA – LI-6262) equipped with a pressure transducer and an auxiliary pump or continuous nitrogen flow for the reference cell. Each IRGA was connected to a gas multiplexer, built and modified to our needs after the concept described in Xu et al. (1999), which allows the measurement of CO_2 concentrations at different levels by the same instrument. The pumps for the transport of the air to the main manifold were operated at a flow rate of 8–10 l min^{-1} and the smaller pumps between the manifold and the IRGA had a flow rate of around 2–3 l min^{-1}. The signals of the IRGA's analog output (CO_2, H_2O and instrument temperature) were measured by a CR23X data logger (CSI, Logan, UT), which also controlled

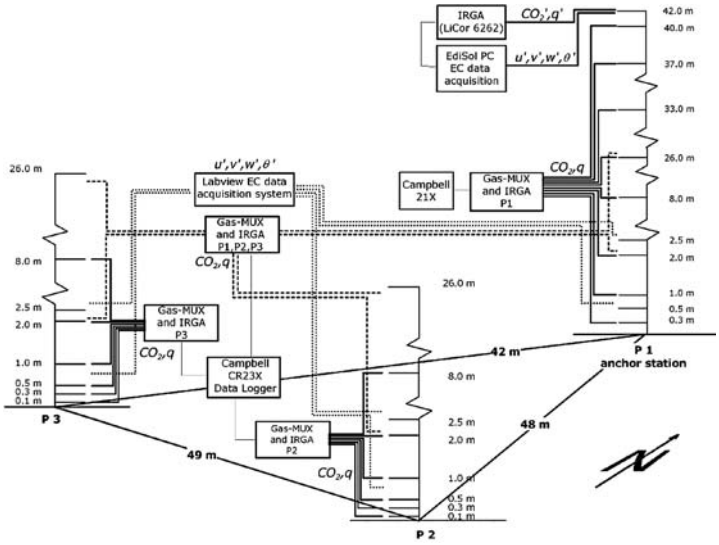

Figure 2. Schematic of experimental set-up: CO_2 profiles at P1, P2 and P3, each on a IRGA gas-multiplexer (solid lines), CO_2 comparison at P1, P2 and P3, all on one IRGA gas-multiplexer (dashed lines), and wind measurements in the trunk space (dotted lines). EC system is at P1 (top at P1).

TABLE I
Instrumentation (only measurements referred to in this study are listed).

Measurement	Location	Instrument	Manufacturer
Fluxes			
3D momentum and sensible heat flux EC	P1, 42 m	Gill Solent R2 #205	Gill Instruments, U.K.
	P1, 0.5 m, 2.5 m	CSAT3 #118, #199	CSI, Logan, UT, U.S.A.
	P2, 0.5 m	Gill Solent R2 #43	Gill Instruments, U.K.
	P2, 2.5 m	Gill HS #46	Gill Instruments, U.K.
	P3, 0.5 m, 2.5 m	Gill Solent R2 #160, #212	Gill Instruments, U.K.
CO_2 and H_2O EC	P1, 42 m	Li-6262 IRG3-#539	LiCor, Lincoln, NE, U.S.A.
Profiles			
CO_2 and H_2O	P1, P2, P3	Li-6262 IRG3 -#381, #315, #1035	LiCor, Lincoln, NE, U.S.A.
CO_2 and H_2O	Comparison of P1, P2, P3	Li-6262 IRG3-#814	LiCor, Lincoln, NE, U.S.A.

EC is eddy covariance.

the switching of the multiplexer valves by three 16-channel AC/DC controllers (SDM-CD16AC, CSI). To reach a constant value for every single CO_2 measurement after switching the respective valve, the sample cell of the gas analyser was purged for 6 s with the ambient air from the respective level tube before taking a measurement. After purging, seven samples were taken during the next 14 s. With this arrangement, one cycle for six measurement levels lasts 2 min and thus, for a half hourly mean value, 15 periods with seven samples each were used for each measurement level. The reference flow path was continuously scrubbed with soda lime and a desiccant ($Mg(ClO_4)_2$); these chemicals were changed when the gas analysers were calibrated. All gas analysers were adjusted for zero offset and span correction at least every 7 days. Additionally zero and span adjustments according to LiCor application note 123 (LiCor, Lincoln, NE, U.S.A.) were applied to the raw data, but had only a small impact. By the redundant measurements at 2 m we were able to compare the four gas analysers with each other. It is shown that by a simple linear regression the data from the different gas analysers can be adjusted to a satisfying accuracy with a standard error of ± 1.1 ppm. Due to a different sampling strategy, the high resolution CO_2 profile at P1 was not comparable to P2 and P3 and the comparison measurements were used to model the profile at P1 during the measurement period. The method of construction of the CO_2 profiles at the boundaries of the control volume (at P1, P2 and P3) using the available data is described in the Appendix. Because CO_2 concentration above the canopy was only measured at P1, the measured value at 40 m is considered to be representative of the CO_2 concentration at the top of the control volume.

4.2. Horizontal CO_2 concentration gradient

The left side of Figure 3 shows an arbitrary example for the height dependent horizontal concentration gradient and the wind profile (which is treated in the next section). From the three concentration profiles, the horizontal CO_2 concentration gradient profile can be calculated by applying the following procedure: for each height z, a plane can be defined by the east and north coordinates of the three edge points P1, P2 and P3 in the x and y direction and the respective concentration values in the z direction. This plane can also be described by a three-dimensional vector, which in our case finally describes the amount (z) and the direction (x, y) of the horizontal concentration gradient for each height level (see Appendix for more details).

The change of amount and direction of the gradient with height requires therefore a three-dimensional treatment to calculate the horizontal advection term. The mean distribution of the measured gradients at 2 and 26 m in Figure 4 shows the expected generally larger gradients in the trunk space

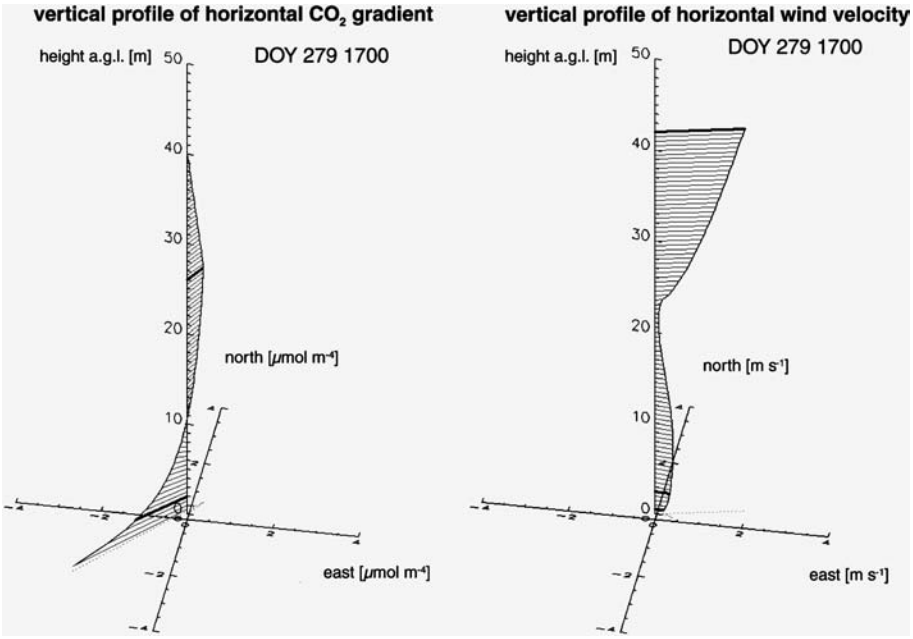

Figure 3. Examples of an arbitrarily chosen 30-min period for the horizontal concentration gradient profile (left) and the wind profile (right). Thick lines denote the measurements at the respective heights. For the derivation of the profiles refer to the Appendix.

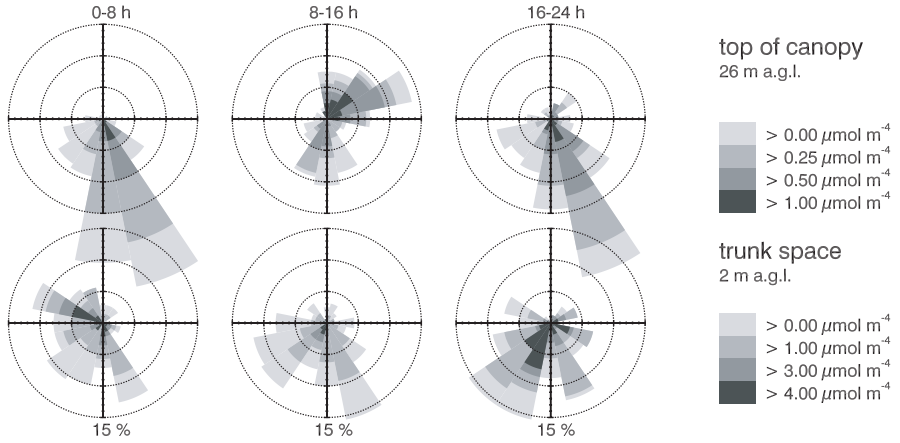

Figure 4. Diurnal gradient field at the top of the canopy (top) and in the trunk space (bottom), pointing from low to high CO_2 concentrations. Outer circles denote 15% of total values.

compared to the top of the canopy. Largest gradients in the sub-plot are observed in the late evening and at night with maxima larger than 4 μmol m^{-4}. The direction of the gradient (pointing from low to high

concentrations) in the trunk space is widely scattered over a 180° sector centered around the south-western direction and shows no clear diurnal trend. A slight tendency to westerly directions in the late night and southerly to south-westerly directions during the day until late evening can be observed. In the sub-plot, concentrations are generally higher in the southern to south-western sector of the control volume at all times. At the top of the canopy, the diurnal pattern is more pronounced with the largest gradients (>1 μmol m^{-4}) occurring during daytime and lower concentrations in the south-western sector, while at night under stable conditions, we have the highest concentrations in the south-eastern sector. This 90° switch of the CO_2 gradient may be related to canopy heterogeneity, i.e., a different stand structure in the south-western sector will cause a larger sink during daytime due to photosynthesis and thus be responsible for the daytime gradients.

4.3. Flow field and vertical wind profile

The derivation of the vertical wind profile from the available data is given in Appendix A. It should only be noted here that for the wind profile below the canopy, wind measurements at the respective level from all three edges of the prism were averaged and the resulting profile is considered to be representative for the whole control volume. The right side of Figure 3 shows an arbitrary chosen profile. Due to the different aerodynamic resistances above, in, and below the canopy, the wind profile shows a relative minimum at the height where the vegetation density is highest. This is simulated by modifying the understorey wind profile with a brake function (for more details see Appendix A). Wind velocities in the trunk space are very low in general and also compared to the top of the main tower at P1. Despite the slight descending terrain to the south, no nightly cold air drainage flows could be observed at the site. Winds are very persistent blowing mainly from the south-western sector both above and below the canopy at all times, as shown in Figure 5. During the day, the wind direction in the trunk space is mostly southerly with contributions from all other sectors.

The mean vertical velocity component has been corrected for sensor tilt using

$$\bar{w}(z_r) = \bar{w}(z_r)_{\text{measured}} - \sqrt{\bar{u}^2(z_r) + \bar{v}^2(z_r)}\tan(a_0 + a_1 \sin(\alpha + a_2)), \tag{9}$$

where α is the wind direction in degrees. Coefficients a_0, a_1 and a_2 were evaluated according to Lee (1998), Baldocchi et al. (2000) and method (1) in Paw U et al. (2000), using a sinusoidal fit of the tilt angle against wind

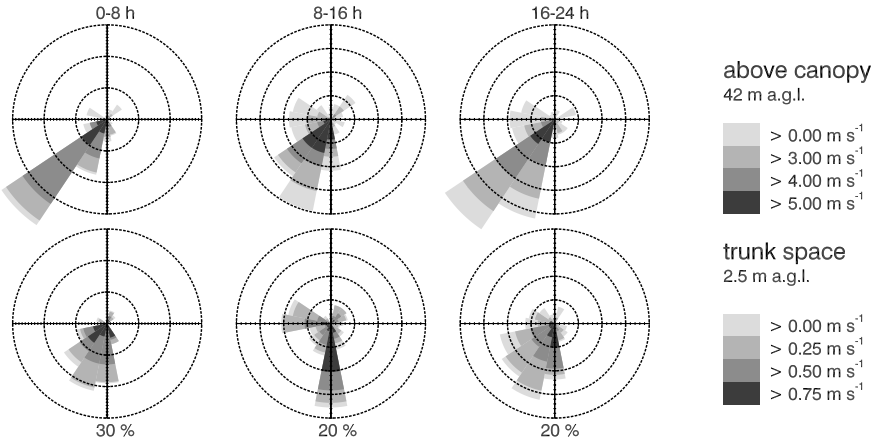

Figure 5. Distribution of wind field above the canopy (top) and in the trunk space (bottom).

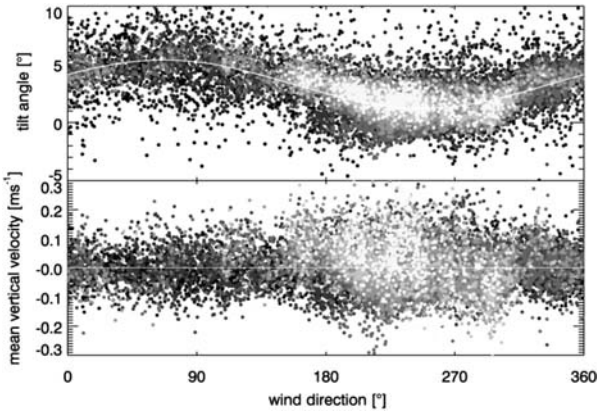

Figure 6. Top: sinusoidal fit (white line) of tilt angle against wind direction for the 2001 dataset from the Gill R2 Sonic at 42 m (half hourly means). Bottom: adjusted mean vertical wind component for the same dataset. Brighter circles refer to higher wind velocities.

direction α for the long-term dataset of the whole year 2001 ($a_0 = 3.3°$ (offset), $a_1 = 2.07°$ (amplitude) and $a_2 = 23.1°$ (phase shift)). Fit and residuals are shown in Figure 6.

5. Results

5.1. Vertical advection

Vertical advection is determined according to Equation (5) by the product of the corrected mean vertical velocity at z_r and the difference between the

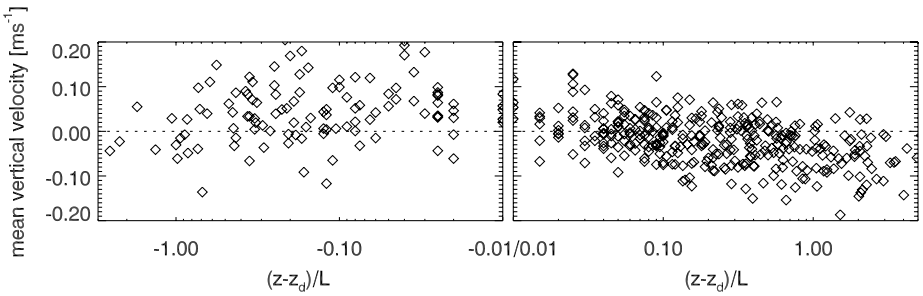

Figure 7. Hourly mean vertical velocity (corrected) at the reference height for the observed stability range from DOY 263 to 283.

concentration at z_r and the mean concentration in the control volume Δc. Figure 7 shows the corrected mean vertical velocity component versus stability index for the observed stability range (with z_d as the zero plane displacement height (=20.3 m) and L as the Obukhov length). During daytime under slightly unstable conditions, w is mainly positive, while under stable conditions at night, negative values dominate.

A closer look at the mean profiles of CO_2 shows the characteristic diurnal course for forest ecosystems: during the night, the forest acts as a source due to the respiration of soil and vegetation and the concentrations continuously decrease with height. After sunrise, when photosynthesis starts, the concentration minimum of the profile moves slowly downward to mid-canopy height from noon until late afternoon as the result of the carbon uptake of the plants. This is shown in Figure 8 where the concentration differences Δc

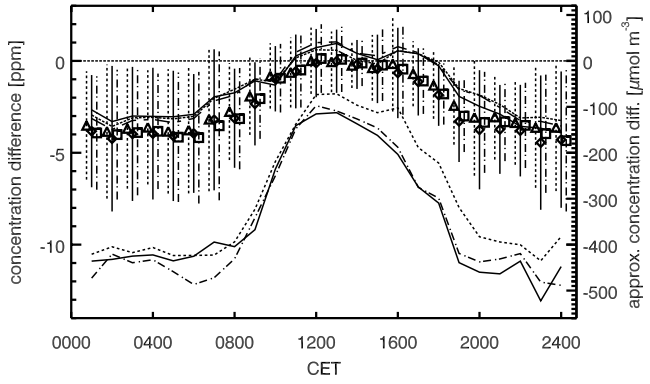

Figure 8. Diurnal course of hourly mean CO_2 concentration differences for DOY 263–283: c(40 m) – c(26 m) (thick lines), c(40 m) – c(2 m) (thin lines) and c(40 m) – $\langle c \rangle$ (symbols with standard error bars) at P1 (dotted, triangles), P2 (solid, diamonds) and P3 (dash-dotted, squares). CET is central European time.

between the reference height and 26 m, 2 m a.g.l. and the mean concentration $\langle c \rangle$ in the layer below the reference height are plotted, as a diurnal course, of hourly means. The scatter is larger at night. As Δc tends to values around zero, vertical advection will be low during daytime as expected, and observed also by Aubinet et al. (2003). During the night, Δc scatters around −4 ppm, which implies a significant loss of CO_2 due to the negative mean vertical velocities under stable conditions shown in Figure 7. The difference of Δc between the three edge points P1, P2 and P3 is very small, and thus the mean value of these three concentration differences is taken as a representative value for the prism control volume and the calculation of the vertical advection term.

From Figures 7 and 8, a first estimate of the mean nightly vertical advection can be made: with nightly mean vertical velocities of −0.05 and −0.1 m s^{-1}, and a concentration difference of around −120 μmol m^{-3}, vertical advection will be 6 and 12 μmol m^{-2} s^{-1} respectively. Air of lower concentration is therefore transported into the control volume by the negative vertical velocity component. This rate is quite high compared to a mean daily maximum EC flux of −11 μmol m^{-2} s^{-1} during the campaign. However, it is obvious from the same figures that the scatter in both variables and thus also in their product is remarkably large. We will see in the next section that vertical advection is partly compensated by the horizontal advection.

5.2. HORIZONTAL ADVECTION

From Figures 4 and 5, several consequences for the estimation of horizontal advection can be derived. The most obvious is that we have to distinguish between the trunk space and canopy layer. In the sub-plot, low wind velocities and large horizontal concentration gradients dominate and the wind direction and the direction of the horizontal gradient are more or less opposite (wind blowing from south-west transports air with a relatively higher CO_2 concentration into the control volume). Supposing a mean wind velocity in the trunk space of 0.4 m s^{-1} and a horizontal gradient component in the opposite direction of the mean flow of 1 μmol m^{-4} results in an advective flux of −4 μmol m^{-2} s^{-1} for a vertical layer of 10 m thickness in the trunk space as a first estimate. In a similar way, advection for the canopy layer can be estimated. Supposing a mean wind speed of 2 m s^{-1} from the south-west, and a horizontal gradient component of 0.1 μmol m^{-4} in the opposite direction, results in an advective flux of around −6 μmol m^{-2} s^{-1} for a layer of 30 m thickness. The magnitude of the advective fluxes is therefore of the same order as the mean daytime maximum of the EC flux.

These simple approximations show that, besides the height of the considered layer, even slight changes in u and v and/or the horizontal gradients

$\partial c/\partial x$ and $\partial c/\partial$y have a significant influence on the result. This is the reason why we tried to investigate the variation of the horizontal advection term with height by constructing vertical profiles of the horizontal wind vector and the horizontal concentration gradient, because it allows a deeper insight into the behaviour of advective processes for the different vertical layers of the forest ecosystem. Figure 9 shows the mean diurnal course of the horizontal non-turbulent advective flux as a function of the height z and the respective integrals (averaging time: 2 h). Between 18 and 24 m, the layer of maximum vegetation density, low wind velocities and small horizontal CO_2 gradients result in very low values for horizontal advection. This is also the height range where the horizontal gradient frequently changes direction, which means a zero crossing of the gradient. Below and above this height, the maximum and minimum advection values are at the top of the canopy (30 m) and right above the ground.

For both layers, we have positive horizontal fluxes during daytime, which means transport of CO_2 out of the control volume. The amount of the positive flux is higher in the crown space and above the canopy than in the trunk space. In the first half of the night, only weak horizontal advection occurs above 20 m a.g.l. while in the trunk space, the large horizontal gradients result in an increasing inflow of CO_2 into the control volume as we approach the ground. As the night proceeds, the inflow of CO_2 also begins in

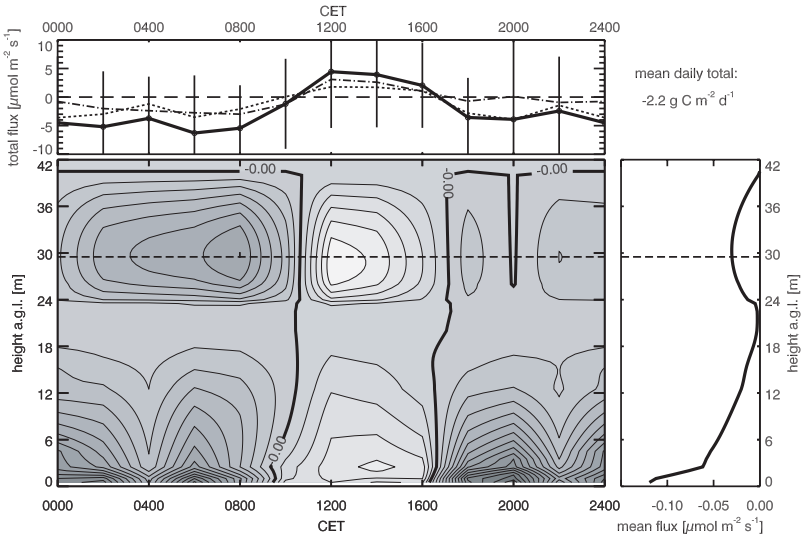

Figure 9. Two-hour averages of non-turbulent horizontal advective flux depending on height and time (contour plot, bright colours refer to positive, dark colours to negative fluxes, contour interval is 0.02 μmol m^{-2} s^{-1}, dashed line indicates the canopy height). Top: total (solid), trunk space (dashed) and crown space (dash-dotted) flux in the control volume. Right: mean daily flux profile.

and above the canopy and the total horizontal advective flux reaches the highest values in the second half of the night.

Our estimate of NEE results in a daily mean carbon uptake of 1.56 gC m^{-2} d^{-1} h; all components are plotted in Figure 10 and Table II gives an overview of the daily totals. The range of the scatter for all variables is similar and generally large.

6. Discussion and Outlook

We are aware of the limited base of the results presented in this paper. The dataset covers only 20 days at the end of a vegetation growth period and the advection terms show large scatter (but this probably will also be the case in a long-term study). The assumptions used to derive the advection terms and the choice of wind profile functions that were applied affect the outcome of

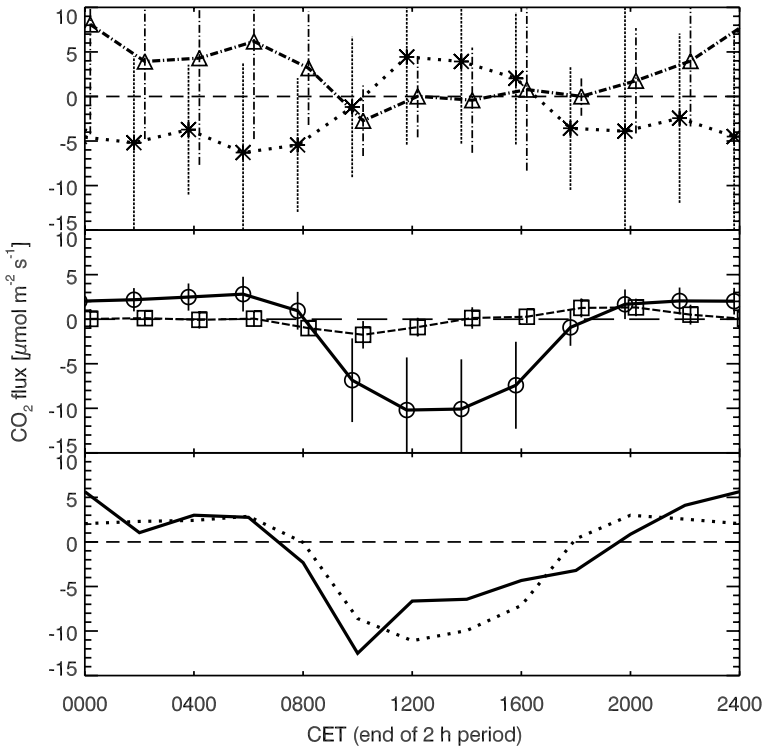

Figure 10. Mean diurnal course of CO_2 fluxes with standard error bars. Top: horizontal advection (dotted, stars) and vertical advection (dashed dotted, triangles); middle: EC flux (solid, circles) and storage change (dashed, squares); bottom: total NEE (all terms, solid) and NEE (EC flux and storage term only, dotted).

TABLE II
Mean sums (DOY 263 – 283) of carbon flux in gC m^{-2} per period of relevant variables for NEE.

Period	EC flux	Storage change	Vertical advection	Horizontal advection	Total
0000–0800	0.73	−0.08	1.52	−1.78	0.39
0800–1600	−3.00	−0.19	−0.20	0.80	−2.59
1600–2400	0.43	0.27	1.19	−1.25	0.64
Total day	−1.84	0.00	2.51	−2.23	−1.56

this study. However, there are only a few comparable studies and they are mostly treated in a two-dimensional manner. These are good reasons why conclusions that would be regarded as generally valid should not be made. However, we are convinced of the consistency of the data and therefore some conclusions can be drawn from the presented analysis.

6.1. Discussion

The opposite sign of horizontal and vertical advection supports the idea that the two fluxes will cancel out each other in the long-term carbon balance. However, the large values of the two fluxes and the large scatter also suggests that there is a large day-to-day variability.

The results presented in Table II show that, during the night (including the transition periods 1600–0800 local time, horizontal and vertical advections are of opposite sign and of the same order of magnitude, which results in a small gain of carbon (0.32 gC m^{-2}) for this period due to advection. During the day (0800–1600) vertical and horizontal advection, though also in opposite directions, do not cancel each other. From 0800 to 1600 horizontal advection reduced the observed carbon sink by about 20%, while vertical advection is almost zero. The reason for this difference between horizontal and vertical advection is the CO_2 gradient, which disappears for daytime conditions in the vertical direction, but prevails in the horizontal direction. For this period and under the specific conditions of the site, this fact may raise the question of whether a possible overestimation of the CO_2 sink might not only be a consequence of the underestimation of the nighttime fluxes under weak turbulent conditions, as has been stated by several investigators, but could also be caused by large horizontal advection (which is not totally compensated by vertical advection) during daytime.

Typically, long-term CO_2 budgets are determined in turbulent periods only by applying the so-called u_* correction (Falge et al., 2001a). For the Tharandt site, a threshold of $u_* > 0.3$ m s^{-1} was derived from long-term nighttime

NEE measurements (Bernhofer et al., 2003a, b). The u_* filtered dataset of the same period in 2001 shows smaller advection terms, but they do not completely disappear. However, the short period of measurements and the low number of remaining data after filtering (40%) does not allow a final conclusion. To investigate the relationship between the effect of the u_* correction and the advection terms on NEE is one of the main goals of the recent long-term advection experiment (from May to October 2003) at the same site.

6.2. Outlook

There are of course still methodological problems and potential deficits in the estimation of the advection terms. Errors in vertical velocity, the vertical profiles of wind velocity and CO_2 concentrations and in the horizontal concentration gradients caused by experimental design and measurement inaccuracies reduce the comparability of the results. Despite these uncertainties, it is obvious that the advection terms should be included at least in some detail in future long-term carbon budgets. Similar advection experiments have to be carried out at different locations and under different conditions, which may lead to a reduction of the errors and will help to define a standard procedure to improve the present methodology for estimating carbon sequestration.

Acknowledgements

We acknowledge the staff of the Institute of Hydrology and Meteorology of the Dresden University of Technology for their support before, during and after the experiment. Special thanks go to Barbara Köstner and Thomas Grünwald for their assistance in administration and data support. Andreas Christen and Irene Lehner from the Institute of Meteorology at the University of Basel did a great job during the initial phase of the experiment. This project is supported by the Bundesministerium für Bildung und Forschung, Germany in the frame of the AFO 2000 project VERTIKO (Contract #07ATF37-UBAS).

Appendix A

1. Vertical wind profile

The vertical wind profile $U(z)$ was constructed from the averaged wind measurements at P1, P2 and P3 at heights $z = \{0.5, 2.5\}$ m and the

measurement at 42 m from the main tower P1. For the above canopy wind profile $U_{\text{high}}(z)$, the following relationships were applied: $u_* = 0.2U(42)$, $z_d = 0.7h$ and $z_0 = 0.08h$, with the profile modified by the usual stability functions (i.e., Panofsky and Dutton, 1984).

The wind profile in the canopy space $U_{\text{low}}(z)$ was calculated using $U_{\text{low}}(z) = a_0 \ln(a_1\ z)$ for $0 < z < (z_d + z_0)$, where the coefficients a_0 and a_1 were directly computed from the average of wind measurements at 0.5 and 2.5 m a.g.l. at P1, P2 and P3. To account for the vertical distribution of roughness within the canopy, the lower wind profile (up to $z_d + z_0$ (= 23 m)) was multiplied by a Gaussian attenuation function (Figure A1). The form of the attenuation function $f(z)$ is (modified after Joss (1996) and Raupach and Thom (1981)):

$$f(z) = 1 - k_0 \exp\left(-k_1^2\left(\frac{z}{z_r} - k_2\right)^2\right) \quad \text{for } 0 < z < (z_d + z_0), \tag{A1}$$

where k_0 refers to the maximum attenuation effect, k_1 is the reciprocal of the normalised length of the crown space and k_2 is the normalised height of the maximum attenuation effect, which corresponds to the height of the highest density of the vegetation. The height for normalisation is the reference height z_r (42 m). For the Tharandt site, the values for $k_{0,1,2}$ are 0.85, 5.0 and 0.5, respectively. The total profile is then composed of the above canopy wind profile and the modified wind profile in the canopy as $U(z) = U_{\text{high}}(z) + f(z)\,U_{low}(z)$.

2. Vertical CO_2 profiles

The measured CO_2 concentration values at $z = \{0.1, 0.3, 0.5., 1.0, 2.0, 8.0, 26.0\}$ m at P2 and P3 were approximated with a quadratic log-function

$$c_{\text{P2,P3}}(z) = a_0 + a_1 \ln(z) + a_2 \ln^2(z), \tag{A2}$$

which was found to fit these high resolution profiles best. Coefficients a_i in Equation (A2) were classified according to their relationship to the concentration difference between 26 and 2 m. If only data from 2 to 26 m were available (which was always the case at P1), the missing values at $z = \{0.1, 0.3, 0.5, 1.0, 8.0\}$ m were modelled using (A2) and the coefficients a_i related to the concentration difference between 26 and 2 m for the respective time period. The measured values (from 2 to 26 m) were weighted 10 times for a second fitting procedure. The measured value at 40 m a.g.l. is supposed to be valid for any horizontal position so concentrations from 26 up to 40 m were linearly interpolated.

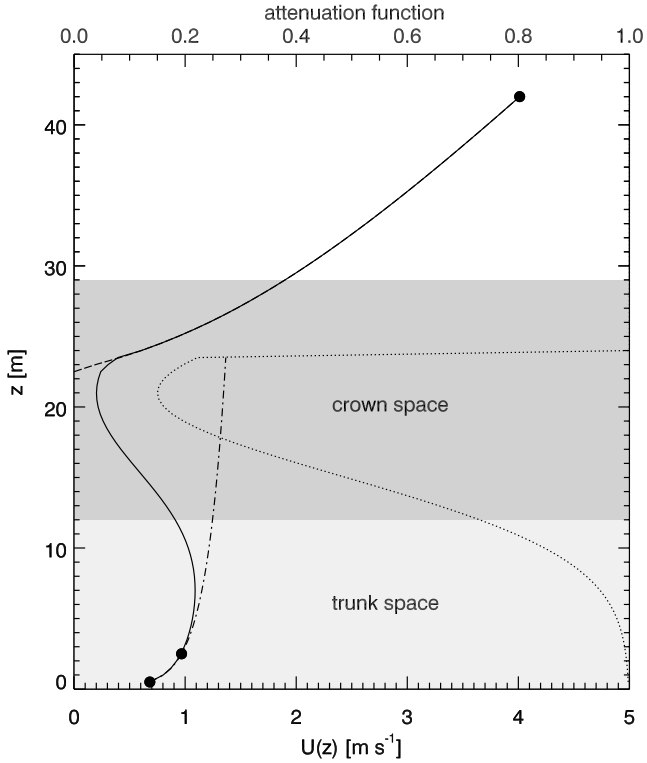

Figure A1. Arbitrarily chosen wind profile (solid) derived from measurements (circles). Upper profile (dashed), lower profile (dash-dotted), brake function (dotted, refers to upper x-axis).

3. Horizontal CO_2 gradient

The vertical profile of horizontal CO_2 gradients is calculated from the plane defined by the CO_2 concentrations $c_{P1}(z)$, $c_{P2}(z)$ and $c_{P3}(z)$ at each edge point P1, P2 and P3 of the prism for a certain height z. These gradients are partitioned each into a north and east component and are considered to be representative for the whole region of interest. Multiplying the associated wind components $u(z)$ and $v(z)$ with the gradients yields the advective flux.

The plane given in Figure A2 is determined by P1($P1_x$, $P1_y$, $P1_z$), P2($P2_x$, $P2_y$, $P2_z$) and P3($P3_x$, $P3_y$, $P3_z$), where the x and y coordinates are given by the experimental set-up and the z coordinates refer to the CO_2 concentrations in units of ppm. Thus

$$\begin{vmatrix} x & P1_x & P2_x & P3_x \\ y & P1_y & P2_y & P3_y \\ z & P1_z & P2_z & P3_z \\ 1 & 1 & 1 & 1 \end{vmatrix} = 0, \tag{A3}$$

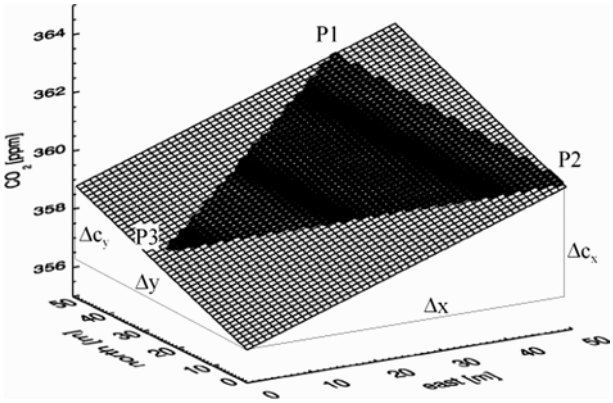

Figure A2. Detailed sketch for a plane defined by arbitrary concentrations of 362, 360 and 358 ppm at locations P1, P2 and P3 respectively.

which results in the equation for the plane $A(z)x + B(z)y + Cz + D(z) = 0$, with

$$A(z) = \mathrm{P2}_y\mathrm{P3}_z + \mathrm{P3}_y\mathrm{P1}_z + \mathrm{P1}_y\mathrm{P2}_z - \mathrm{P3}_y\mathrm{P2}_z - \mathrm{P1}_y\mathrm{P3}_z - \mathrm{P2}_y\mathrm{P1}_z,$$

$$B(z) = \mathrm{P3}_x\mathrm{P2}_z + \mathrm{P1}_x\mathrm{P3}_z + \mathrm{P2}_x\mathrm{P3}_z - \mathrm{P2}_x\mathrm{P3}_z - \mathrm{P2}_x\mathrm{P1}_z - \mathrm{P1}_x\mathrm{P2}_z,$$

$$C = \mathrm{P2}_x\mathrm{P3}_y + \mathrm{P3}_x\mathrm{P1}_y + \mathrm{P1}_x\mathrm{P2}_y - \mathrm{P3}_x\mathrm{P2}_y - \mathrm{P1}_x\mathrm{P3}_y - \mathrm{P2}_x\mathrm{P1}_y = \text{constant},$$

$$D(z) = \mathrm{P1}_x\mathrm{P3}_y\mathrm{P2}_z + \mathrm{P2}_x\mathrm{P1}_y\mathrm{P3}_z + \mathrm{P3}_x\mathrm{P2}_y\mathrm{P1}_z - \mathrm{P1}_x\mathrm{P2}_y\mathrm{P3}_z - \mathrm{P3}_x\mathrm{P1}_y\mathrm{P2}_z - \mathrm{P2}_x\mathrm{P3}_y\mathrm{P1}_z,$$

and finally the x (east) and y (north) components

$$\frac{\partial \bar{c}(z)}{\partial x} = \frac{A(z)}{C} \quad \text{and} \quad \frac{\partial \bar{c}(z)}{\partial y} = \frac{B(z)}{C} \tag{A4}$$

in units of ppm m^{-1}.

4. Error analysis

There are three main sources of errors for the advection terms, namely the vertical wind profile, the mean vertical wind component and the horizontal CO_2 concentration gradient.

As described above, the wind profile was constructed using only three measurement heights. First, the two values in the trunk space are averages of the three measurements at P1, P2 und P3. Variation of wind velocity from averaging is ± 0.09 and ± 0.07 m s^{-1} and the standard deviation of the wind direction is ± 12 and ± 8 degrees for the 0.5 m and the 2.5 m levels, respectively. Secondly, one may question whether the brake function modifies the

profile in a realistic manner. Measurements at $z = \{2, 8, 18, 26, 33\}$ m from the 2003 campaign, however, show that the modelled profile represents the conditions very well and the height and the amount of the maximum brake effect have been confirmed by these measurements. Instrument accuracy as given by the manufacturers is around $\pm 3\%$ for ultrasonic anemometers. Sampling errors for the mean horizontal velocity are negligible at averaging times of 120 min at 20 Hz.

The mean vertical velocity sampling error can be estimated after Wilczak et al. (2001), and for the Tharandt site this results in an error of 0.01 m s^{-1} for neutral to stable and 0.02 m s^{-1} for unstable conditions for the two-hourly means. These values are well in the range of reported errors for surface-layer datasets. The sinusoidal fit procedure corrects the mean vertical velocity component mainly for errors due to instrument tilt and local terrain effects with reference to the long-term data record. The remaining residual results from e.g. convection or local flows due to thermal effects (Lee et al., 1998). The coordinate rotation is therefore a tool to remove systematic errors resulting from the experimental set-up and the specific topographic conditions of the site and should not induce additional errors.

Horizontal profiles at P1, P2 and P3 are constructed from two measurements at 2 and 26 m heights and a log-square function, which was found to fit best the single high resolution profiles, using a look-up table for the coefficients a_0, a_1 and a_2 depending on the concentration difference between 2 and 26 m. This means that the error of the single profiles is the same, and will cancel out when calculating horizontal gradients. The remaining error comes from sampling uncertainties and the accuracy of the instrument, since the 2 and 26 m values were measured by the same IRGA (#841). Sampling errors are negligible if we use two-hourly averages for the calculation of the advection terms. CO_2 analyzer accuracy is given as ± 1 ppm at 350 ppm by the manufacturer; no bias error as described in Aubinet et al. (2003) was observed in our data. Comparing the measured horizontal gradients at heights of 2 and 26 m with the gradients calculated from the constructed profiles at the same heights results in a mean standard error of ± 0.4 and ± 0.04 μmol m^{-4}, respectively. The larger error in the trunk space results from the higher fluctuations of the CO_2 concentrations.

Using the normalised peak frequency of 0.063 for the power spectrum of a scalar from Kaimal et al. (1972) for neutral conditions, and assuming a horizontal wind velocity of 3 m s^{-1} for the layer above the canopy and a velocity of 0.6 m s^{-1} for the trunk space, results in a characteristic length scale of 20 and 90 m, respectively, applying Taylor's hypothesis. Thus the distance of about 50 m between the towers is a good choice for which to measure representative horizontal gradients.

These considerations lead to an absolute error for the vertical advection term of about ± 2.5 μmol m^{-2} s^{-1} and of about ± 3 μmol m^{-2} s^{-1} for the

horizontal advection term. Considering the large day-to-day variability, these errors should have only a small influence on the averaged diurnal course of the advective terms shown in Figure 10.

References

Aubinet, M., Chermanne, B., Vandenhaude, M., Longdoz, B., Yernaux, M., and Laitat, E.: 2001, 'Long Term Carbon Dioxide Exchange above a Mixed Forest in the Belgian Ardennes', *Agric. For. Meteorol.* **108**, 293–315.

Aubinet, M., Grelle, A., Ibrom, A., Rannik, U., Moncrieff, J., Foken, T., Kowalski, A. S., Martin, P. H., Berbigier, P., Bernhofer, C., Clement, R., Elbers, J., Granier, A., Grünwald, T., Morgenstern, K., Pilegaard, K., Rebmann, C., Snijders, W., Valentini, R., and Vesala, T.: 2000, 'Estimates of the Annual Net Carbon and Water Exchange of Forests: The EUROFLUX Methodology', *Adv. Ecol. Res.* **30**, 113–175.

Aubinet, M., Heinesch, B., and Yernaux, M.: 2003, 'Horizontal and Vertical CO_2 Advection in a Sloping Forest', *Boundary-Layer Meteorol.* **108**, 397–417.

Baldocchi, D., Finnigan, J. J., Wilson, K., Paw U, K. T., and Falge, E.: 2000, 'On Measuring Net Ecosystem Exchange over Tall Vegetation on Complex Terrain', *Boundary-Layer Meteorol.* **96**, 257–291.

Baldocchi, D., Vogel, C., and Hall, B.: 1997, 'Seasonal Variation of Carbon Dioxide Exchange Rates above and below a Boreal Jack Pine Forest', *Agric. For. Meteorol.* **83**, 147–170.

Bernhofer, C. and Vogt, R.: 1999, 'Energy Balance Closure Gaps – A Methodical Problem of Eddy Covariance Measurements?', in R. J. Dear, J. D. Kalma, T. R. Oke, and A. Auliciems (eds.), *Biometeorology and Urban Climatology at the Turn of the Millennium*: *Selected Papers from the Conference ICB-ICUC'99* (*Sydney*, *8–12. November 1999*), pp. 199–203.

Bernhofer, C., Feigenwinter, C., Grünwald, T., and Vogt, R.: 2003a, 'Spectral Correction of Water and Carbon Flux for EC Measurements at the Anchor Station Tharandt', in C. Bernhofer (ed.), *Tharandter Klimaprotokolle*, Vol. 8, Dresden University of Technology, Dresden, pp. 1–13.

Bernhofer, C., Aubinet, M., Clement, R., Grelle, A., Grünwald, T., Ibrom, A., Jarvis, P., Rebmann, C., Schulze, E.-D., and Tenhunen, J. D.: 2003b, 'Spruce Forests (Norway and Sitka Spruce, Including Douglas Fir): Carbon and Water Fluxes, Balances, Ecological and Ecophysiological Determinants', in R. Valentini, (ed.), *Fluxes of Carbon*, *Water and Energy of European Forests*, *Ecological Studies*, Vol. 163, Springer, Berlin, pp. 99–123.

Dolman, A. J., Moors, E. J., and Elbers, J. A.: 2002, 'The Carbon Uptake of a Mid Latitude Pine Forest Growing on Sandy Soil', *Agric. For. Meteorol.* **111**, 157–170.

Eugster, W. and Siegrist, F.: 2000, 'The Influence of Nocturnal CO_2 Advection on CO_2 Flux Measurements', *Basic Appl. Ecol.* **1**, 177–188.

Falge, E., Baldocchi, D. D., Olson, R. J., Anthoni, P., Aubinet, M., Bernhofer, C., Burba, G., Ceulemans, R., Clement, T., Dolman, H., Granier, A., Gross, P., Grünwald, T., Meyers, B. E., Moncrieff, J., Moors, E., Munger, J. W., Pilegaard, K., Rannik, U., Tebmann, C., Suyker, A., Tenhunen, J., Tu, K., Verma, S., Vesala, T., Wilson, K., and Wofsy, S.: 2001a, 'Gap Filling Strategies for Defensible Annual Sums of Net Ecosystem Exchange', *Agric. For. Meteorol.* **107**, 43–69.

Falge, E., Baldocchi, D. D., Olson, R. J., Anthoni, P., Aubinet, M., Bernhofer, C., Burba, G., Ceulemans, R., Clement, T., Dolman, H., Granier, A., Gross, P., Grünwald, T., Meyers, B. E., Moncrieff, J., Moors, E., Munger, J. W., Pilegaard, K., Rannik, U., Tebmann, C., Suyker, A., Tenhunen, J., Tu, K., Verma, S., Vesala, T., Wilson, K., and Wofsy, S.: 2001b,

'Gap Filling Strategies for Longterm Energy Flux Data Sets', *Agric. For. Meteorol.* **107**, 71–77.

Finnigan, J. J.: 1999, 'A Comment on the Paper by Lee (1998): "On Micrometeorological Observations of Surface-Air Exchange over Tall Vegetation"', *Agric. For. Meteorol.* **97**, 55–64.

Finnigan, J. J., Clement, R., Malhi, Y., Leuning, R., and Cleugh, H. A.: 2003, 'A Re-evaluation of Long-term Flux Measurement Techniques. Part I: Averaging" and Coordinate Rotation', *Boundary-Layer Meteorol.* **107**, 1–48.

Goulden, M. L., Munger, J. W., Fal, S. -M., Daube, B. C., and Wofsy, S. C.: 1996, 'Measurements of Carbon Sequestration by Long-Term Eddy Covariance: Methods and a Critical Evaluation of Accuracy', *Global Change Biol.* **2**, 183–197.

Grünwald, T.: 2002, *Langfristige Beobachtungen von Kohlendioxidflüssen mittels Eddy-Kovarianz-Technik über einem Altfichtenbestand im Tharandter Wald*, Ph.D. Thesis, Dresden University of Technology, Dresden, Germany, 141 pp.

Grünwald, T. and Bernhofer, C.: 2000, 'Data Gap Filling with Regression Modelling', in R. J. M. Ceulemans, F. Veroustraete, V. Gond, and J. B. H. F. Van Rensbergen (eds.), *Forest Ecosystem Modelling*, *Upscaling and Remote Sensing*, SPB Academic Publishing, The Hague, Netherlands, pp. 61–67.

Joss, U.: 1996, 'Mikrometeorologie, Profile und Flüsse von CO_2, H_2O und O_3 in zwei mitteleuropäischen Nadelwäldern', in E. Parlow (ed.), *Stratus*, Vol. 4, Department of Geography, University of Basel, Switzerland, 100 pp.

Lee, X.: 1998, 'On Micrometeorological Observations of Surface-Air Exchange over Tall Vegetation', *Agric. For. Meteorol.* **91**, 39–49.

Lee, X. and Hu, X.: 2002, 'Forest-air Fluxes of Carbon, Water and Energy over Non-Flat Terrain', *Boundary-Layer Meteorol.* **102**, 277–301.

Leuning, R. and Moncrieff, J.: 1990, 'Eddy Covariance CO_2 Flux Measurements Using Open- and Closed-Path CO_2 Analysers: Corrections for Analyser Watervapour Sensitivity and Damping of Fluctuations in Air Sampling Tubes', *Boundary-Layer Meteorol.* **53**, 63–76.

Massmann, W. and Lee, X.: 2002, 'Eddy Covariance Flux Corrections and Uncertainties in Long-Term Studies of Carbon and Energy Exchanges', *Agric. For. Meteorol.* **113**, 121–144.

Moncrieff, J., Massheder, J., de Bruin, H., Elbers, J., Friborg, T., Heusinkveld, B., Kabat, P., Scott, S., Soegaard, H., and Verhoef, A.: 1997, 'A System to Measure Surface Fluxes of Momentum, Sensible Heat, Water Vapour and Carbon dioxide', *J. Hydrol.* **188–189**, 589–611.

Panofsky, H.A. and Dutton, J. A.: 1984, *Atmospheric Turbulence*: *Models and Methods for Engineering Applications*, John Wiley & Sons, New York, 397 pp.

Paw U, K. T., Baldocchi, D., Meyers, T.P., and Wilson, K. B.: 2000, 'Correction of Eddy-Covariance Measurement Incorporating Both Advective Effects and Density Fluxes', *Boundary-Layer Meteorol.* **97**, 487–511.

Raupach, M.R. and Thom, A. S.: 1981, 'Turbulence in and above Plant Canopies', *Annu. Rev. Fluid Mech.* **13**, 97–129.

Saigusa, N., Yamamoto, S., Murayama, S., Kondo, H., and Nishimura, N.: 2002, 'Gross Primary Production and Net Ecosystem Exchange of a Cool-Temperate Deciduous Forest Estimated by the Eddy Covariance Method', *Agric. For. Meteorol.* **112**, 203–215.

Valentini, R., de Angelis, P., Matteucci, G., Monaco, R., Dore, S., and Scarascia Mignozza, G. E.: 1996, 'Seasonal Net Carbon Dioxide Exchange of a Beech Forest with the Atmosphere', *Global Change Biol.* **2**, 199–207.

Valentini, R., Matteucci, G., Dolman, H., Schultze, E. -D., Rebmann, C., Moors, E. J., Granier, A., Gross, P., Jensen, N. O., Pilegaard, K., Lindroth, A., Grelle, A., Bernhofer, C., Grünwald, T., Aubinet, M., Ceulemans, R., Kowalsky, A. S., Vesala, T., Rannik, U., Berbigier, P., Lousteau, D., Guomundsson, J., Thorgeirsson, H., Ibrom, A., Morgenstern,

K., Clement, R., Moncrieff, J., Montagnani, L., Minerbi, S., and Jarvis, P.G.: 2000, 'Respiration as the Main Determinant of Carbon Balance in European Forests', *Nature* **404**, 861–865.

Wilczak, J. M., Oncley, S. P., and Stage, S. A.: 2001, 'Sonic Anemometer Tilt Correction Algorithms', *Boundary-Layer Meteorol.* **99**, 127–150.

Wofsy, S. C., Goulden, M. L., Munger, J. W., Fan, S. -M., Bakwin, P. S., Daube, B. C., Bassow, S. L., and Bazzaz, F. A.: 1993, 'Net Exchange of CO_2 in a Mid-Latitude Forest', *Science* **260**, 1314–1317.

Xu, L. -K., Matista, A. A., and Hsiao, T. C.: 1999, 'A Technique for Measuring CO_2 and Water Vapour Profiles within and above Plant Canopies over Short Periods', *Agric. For. Meteorol.* **94**, 1–12.